UC San Diego
UC San Diego Electronic Theses and Dissertations

Title

Up-regulation of chemokine receptor-like 2 in an in vitro model of cerebral ischemia

Permalink

Author

Chen, Alice

Publication Date

2011

Peer reviewed|Thesis/dissertation

UNIVERSITY OF CALIFORNIA, SAN DIEGO

**Up-regulation of Chemokine receptor-like 2 in an in vitro model of cerebral
ischemia**

A thesis submitted in partial satisfaction of the

requirements for the degree Master of Science

in

Biology

by

Alice Chen

Committee in charge:

      Professor Gabriel Haddad, Chair
      Professor Raffi Aroian, Co-Chair
      Professor Jean Wang
      Professor Hang Yao
      Professor Elina Zuniga

2011

The Thesis of Alice Chen is approved, and it is acceptable in quality and form for publication on microfilm and electronically:

_____

_____

_____

_____

Co-Chair

_____

Chair

University of California, San Diego

2011

Dedication

I dedicate this thesis to my family, to my mother and father, to my little brother for their unending support and love.

Table of Contents

List of Tables and Figures

ABSTRACT OF THE THESIS

Up-regulation of Chemokine receptor-like 2 in an in vitro model of cerebral
ischemia

by

Alice Chen

Master of Science in Biology

University of California, San Diego, 2011

Professor Gabriel Haddad, Chair

Ischemic stroke is a condition characterized by loss of brain function due
to interruption of blood supply to the brain. A central core of dead cells, the
infarct, forms and expands over time. Thus, the extent of ischemic injury is not
defined immediately following the stroke event. Prevention of lesion expansion

can then limit neurological deficit, making determination of the mechanism of ischemia-induced cell death of great importance.

Using an *in vitro* model of the penumbral rim, the dynamic border between the dead cells of the infarct core and the unaffected healthy tissue, we studied the expression of CCRL2 in relation to ischemic cell death via potential intracellular mediators. CCRL2 is a novel chemokine receptor, previously reported to have no signaling function. However, CCRL2 has yet to be studied in an ischemic context, and a microarray of mouse brain tissue slices treated with IS for 2 hours, reveal CCRL2 to be one of the most highly up-regulated genes.

Western blots reveal CCRL2 to be up-regulated after 14 hours of IS treatment along with JNK and activated caspase-3, a hallmark of apoptotic cell death. In CCRL2-deficient murine tissue, the level of activated caspase-3 decreases to half of the level in wild-type tissue. Additionally, PI staining shows significantly less PI uptake in CCRL2 KO tissue, denoting less cell death, suggesting CCRL2 promotes cell death in ischemia. *In vivo*, CCRL2 was found to be expressed on neurons subjected to MCAO, but not expressed on astrocytes an microglia.

I:

Introduction

Cerebral ischemia and the penumbral rim

Ischemic stroke is a leading cause of death in the modern world. This condition is characterized by a loss of blood flow to the brain due to blockage such as thrombosis or arterial embolism. Once ischemic insult occurs, the affected areas rapidly become hypoxic and hypoglycemic. Damage to brain tissue is a direct result of glutamate excitotoxicity coupled with severe reduction of oxygen and glucose levels which quickly leads to a loss of cellular function and resultant necrotic and apoptotic cell death. The initial lesion, or infarct, is followed by a second period of tissue damage in the penumbra due to ongoing excitotoxicity, spreading depolarization, apoptosis, and inflammation, in which the infarct area expands the longer the stroke is left untreated. This progressive expansion is defined by the recruitment of healthy cells into the ischemic penumbral tissue. Thus, limitation of lesion expansion in the dynamic penumbra can be expected to limit the neurological deficit via neuronal rescue and survival. To this end, an understanding of the mechanisms of cell death in the dynamic infarct rim is important for development of future therapies.

Previous studies have suggested that cell fate in the infarct rim is related to events in the ischemic infarct core (Back et al. 2004, Fisher 2004). The restriction in blood supply caused by a stroke incident causes cells in the area directly fed by the blocked blood vessel to die quickly and form an infarct core. Dramatic biochemical changes occur in this area that can be harmful to adjacent cells which form a distinct area separating the dead cells of the core from the

unaffected healthy tissue. The microenvironment of this infarct rim is characterized by hypoxia, hypercapnia, hypoglycemia, acidosis, ionic shift, and glutamate release (Yao et al. 2007).

An *in vitro* model of ischemic stroke

An *in vitro* model of ischemic stroke has been developed using an ischemic solution (IS) to mimic the pathological environment in the ischemic infarct rim (Yao et al. 2007). The model accounts for ionic disturbances in potassium, sodium, chlorine, calcium; glutamate toxicity; hypoglycemia; hypoxia; and acidosis as a result of altered carbon dioxide, bicarbonate, and hydrogen concentrations (Table 1). Exposure of hippocampal slices to IS for increasing time periods shows a progressive increase in propidium iodide (PI) fluorescence denoting increased cell death (Figure 1), serving to validate the *in vitro* model. PI staining is used to differentiate between necrotic, apoptotic, and normal cells by binding to DNA, intercalating between the bases with little or no sequence preference. This study uses cortical slices rather than hippocampal slices due to the location of the infarct rim in the cortex. This *in vitro* model allows control of the cellular environment and easier interpretation of results. *In vivo*, the complexity of the procedure to stimulate an artificial stroke event as well as physiological differences between mice makes obtaining consistent infarct core size across many samples difficult. Thus the size of the infarct rim differs and makes isolation of the infarct rim and minimizing the amount of the infarct core

and healthy tissue extracted along with rim tissue difficult. In light of such difficulties, the *in vitro* model makes it possible to obtain samples with consistent cellular constituency.

A role for (C-C motif) chemokine receptor-like 2 (CCRL2) in ischemic stroke

(C-C motif) chemokine receptor-like 2 (CCRL2) is an orphan G-protein coupled receptor with seven transmembrane domains. Expression of CCRL2 was found on many human hematopoietic cells including monocytes, macrophages, T-cells, mast cells, astrocytes, microglia, NK cells, and CD34+ progenitor cells. The levels of expression of CCRL2 on these cell types generally increased in response to elements of inflammation including IL-2, LPS, IFN-γ, CD40L (Yoshimura et al. 2010).

The over 40% conserved amino acid identity as well as the close proximity of the CCRL2 gene to other functional chemokine receptors genes suggests CCRL2 is related to the family of signal transducing chemokine receptors. However, other studies have suggested CCRL2 functions as an atypical chemokine receptor by binding to chemokines but not transducing signals. CCRL2 lacks the conserved DRYLAIV motif in the second intracellular loop and instead has the sequence QRYRVSF. Other related GPCRs such as DARC (Duffy antigen), D6, and CCX-CKR (chemocentrix chemokine receptors) lack this conserved motif and while able to bind chemokines, do not transduce signals for

cell migration or intracellular calcium mobilization (Yoshimura et. al. 2010). Instead, these "silent" receptors act to clear chemokines, acting in an anti-inflammatory fashion. CCRL2, when activated by the chemokine RANTES/CCL5, neither calcium mobilization nor cellular migration was induced. However, other studies have shown CCRL2 to play a role in the trafficking of activated, antigen-loaded dendritic cells to lymph nodes, acting in a proinflammatory manner (Otera et. al. 2010).

A study by **Zabel et. al**. showed that mouse CCRL2 was constitutively expressed on mast cells and served to amplify inflammatory responses. Chemerin, a chemoattractant molecule, is a known ligand of CMKLR1 but was also found to bind CCRL2 (Zabel et. al. 2008). Though CCRL2 binds chemerin, ligand binding failed to induce chemotaxis, intracellular calcium mobilization, CCRL2 internalization, or any other functional response. Thus, CCRL2 appears to concentrate chemerin at inflammatory sites to facilitate CMKLR1 binding on adjacent cells (Zabel et. al. 2008).

Whatever the case, CCRL2 appears to have an important role in inflammation. As many components involved in immunity and inflammation play a role in stroke pathology, the role of CCRL2 in focal ischemia proves interesting. In a microarray of brain slices incubated in IS for 2 hours, CCRL2 was found to be one of the highest up-regulated elements (Table 2). CCRL2 is a novel molecule and study of its function in the context of ischemia has yet to be studied. Knowing stroke pathology is characterized by massive cell death, the

question arises: what role, if any, does CCRL2 play in cerebral ischemia-induced

cell death?

II:

RESULTS

IS induces both CCRL2 mRNA and protein expression

To determine the temporal expression of CCRL2 protein, assessment of CCRL2 mRNA expression was first performed at various time points. Cortical slices from mouse neonates were cultured for two weeks prior to incubation in IS or ACSF (control) solution. Tissues that were exposed to 2 or 6 hours of IS showed similar levels of CCRL2 mRNA expression. In contrast, when cortical tissue slices were exposed to 12 hours of IS, CCRL2 mRNA showed a large 35-fold increase (Figure 2a). From this data, protein expression was examined after 14 hours of IS treatment to allow time for protein translation.

Western blots show that CCRL2 protein expression increased 2-fold in cortical tissue after 14 hours of IS treatment compared to control tissue (Figure 2b). Taken together, the data indicates in this *in vitro* model of cerebral ischemia, CCRL2 expression is significantly increased. Whether or not CCRL2 expression contributes to the ischemic cell death will be explored further in this study.

Caspase-3 and c-JUN (N-terminal) kinase (JNK) expression are up-regulated after IS treatment

To assess the contribution of caspase signaling to cell death triggered by ischemia, the proteolytic activity of caspase-3 was analyzed. Caspase-3 was selected because it is a known hallmark of apoptotic cell death and a previous study has shown an increase in activated caspase-3 as a sign of apoptotic

neurons and glial cells (Mogoantă et. al. 2010). Western blots showed cleaved caspase-3 was increased after 14 hours of IS treatment, indicating apoptotic cell death composes a significant portion of ischemic damage (Figure 3a).

c-JUN kinase (JNK) is a key modulator of apoptosis, shown to be involved in promoting apoptosis in neurons after cerebral ischemia (Li et. al. 2010). To analyze a possible connection between CCRL2 and caspase-3, JNK signaling was studied as a possible mediator between the two. Western blots showed activated JNK increased after 14 hours of IS treatment (Figure 4a). In wild-type tissue after 2 hours of IS treatment, there is little change in the activated JNK between IS and ACSF-treated; however, in mutant tissue, a significant decrease is seen after IS treatment (Figure 4b, c). The increase in CCRL2, cleaved caspase-3, and activated JNK suggests a common goal in promoting cell death after ischemic insult.

CCRL2 is directly linked to ischemic cell death

Cortical tissue from CCRL2 knock-out mice were cultured and cell death was quantified. Using PI stain, wild-type and mutant slices were imaged at 0, 8, and 24 hours. At 8 and 24 hours, PI uptake was significantly less in mutant tissue, denoting less cell death in mutant tissue compared to wild-type tissue (Figure 5). Activated caspase-3 was increased in CCRL2 KO tissue, similar to wild-type tissue. However, while wild-type tissue showed a 6-fold increase in

activated caspase-3 after IS treatment, activated caspase-3 was halved with mutant tissue showing a 3-fold increase after IS treatment, both are compared to same type tissue after ACSF treatment (Figure 3). This data suggests CCRL2 plays a direct role in mediating apoptotic cell death in response to ischemia and that caspase-3 plays a role. In addition, Western blots showed JNK signaling decreased in mutant tissue after 2 hours of IS treatment compared to mutant tissue after ACSF treatment. CCRL2 does not appear to mediate all apoptotic cell death, but is still a significant contributor towards ischemia-induced tissue damage.

Chemerin and CMKLR1 are increased after IS treatment

To help further clarify the role CCRL2 plays in ischemia-induced cell death, the activity of chemerin and CMKLR1 were studied. Chemerin is a 15kDa protein ligand shown to bind to CMKLR1 and CCRL2. Binding of chemerin to its receptor promotes chemotaxis of macrophages and dendritic cells to sites of inflammation. CMKLR1 (also known as CCRL1) is a receptor known to play a role in chemotaxis of immune cells along with chemerin. Yoshimura et. al. have shown that chemerin is a ligand for CMKLR1 as well as CCRL2. In this study, to assess if chemerin and CMKLR1 played a role in ischemic cell death, Western blots were analyzed for expression levels. After 14 hours of IS treatment, chemerin was significantly increased in wild-type tissue (Figure 6a). Western blots also showed CMKLR1 was significantly increased in wild-type tissue after

14 hours of IS treatment, suggesting a role for chemerin and CMKLR1 in ischemic cell death (Figure 6b).

CCRL2 is expressed on neurons

To help clarify how CCRL2 contributes to ischemia-induced cell death, the location of CCRL2 is important to identify if the mechanism is cell-type-specific. Immunofluorescence showed CCRL2 to be expressed on neurons, but not on astrocytes or microglial cells (Figure 7). Previous studies have shown CCRL2 to be expressed on immune cells such as mast cells and differentiated B cells, but in this study, CCRL2 is found to be expressed on neurons which is not an immune cell.

III:

Discussion

In this study, I have analyzed the contribution, if any, of CCRL2, an orphan chemokine receptor reported to have no signaling function, to cerebral ischemia-induced apoptotic cell death. Through protein analysis of both wild-type and mutant cerebral tissue, I have shown that CCRL2 has a role in promoting cell death in an *in vitro* model of cerebral ischemia. I have also shown activated, phosphorylated, c-JUN kinase might serve as a signaling intermediate between CCRL2 and the apoptotic cell death signaling cascade. Lastly, I have shown potential roles for chemerin, the chemoattractant protein ligand for CCRL2 and CMKLR1, and CMKLR1in cerebral ischemia and that finally, CCRL2 is expressed on neurons.

CCRL2 and ischemia-induced cell death

Both microarray and RT-PCR (Table 2, Figure 2a) have shown the increased production of CCRL2 mRNA in response to treatment with IS, suggesting a role for CCRL2 protein in the response to ischemia. Western blots confirmed that levels of CCRL2 protein were indeed up-regulated in wild-type tissue in response to IS, and revealed levels of activated caspase-3, a hallmark of apoptotic cell death, were increased as well. Analysis of CCRL2 knock-out tissue showed that while activated caspase-3 did increase in mutant slices, the increase was only half of the increase in wild-type tissue. This data suggests not only is activated caspase-3 the signaler of apoptotic cell death in the penumbral rim, but also CCRL2 somehow contributes to this signaling. While activated

caspase-3 may signal apoptotic cell death, its presence does not guarantee apoptotic cell death. In other words, the level of activated caspase-3 does not equal the amount of apoptotic cell death. To this end, I used PI staining in mutant tissue which confirmed that the absence of CCRL2 corresponded to a decrease in IS-induced injury. It is important to note that PI staining is useful to distinguish between necrotic and apoptotic cell death by primarily staining apoptotic cells, however, this division blurs in long-term cell cultures (Lecoeur et. al. 2008). While the PI staining showed up to 24 hours of IS treatment, which can be considered long-term, the decrease in IS-induced cell death can already be seen at 12 hours. Some cell death can be seen in ACSF-treated tissue, but can be attributed to minimal damage incurred during collection of tissue slices.

An alternate explanation for the data or at least a point of contention might be the inconsistency of the actin bands, which serve as a loading control to ensure all lanes contain the same amount of protein. The decrease in actin between IS-treated and ACSF-treated samples is most likely due to my protein quantification method which does not distinguish between intact and degraded protein, while the actin antibody does. However, since all bands are standardized to the actin bands, the increases and decreases found are accurate and significant. Additionally, Figure 4a shows total JNK at 14 hours of treatment, which should also be found in consistent amounts, shows a difference between IS and ACSF-treated samples similar to that of actin. Figure 4b, c then shows total JNK at 2 hours to have little difference between IS and ACSF-treated

samples. Thus, the discrepancy in actin levels at 14 hours is not due to my methods, but rather to protein degradation, but still serves its role in the normalization of protein levels.

I have shown activated caspase-3 contributes to the signaling of apoptosis and that CCRL2 promotes cell death during ischemic insult. Whether CCRL2 and caspase-3 are linked is difficult to say at this point. Further work is necessary to elucidate the connection, if any, between CCRL2 and caspase-3.

Phosphorylated JNK and ischemia-induced signaling

JNK is known to have a pro-apoptotic signaling function and was therefore a prime candidate as a potential intermediate between CCRL2 and caspase-3. From the data presented in this study, JNK protein is up-regulated in wild-type tissue after 14 hours of IS treatment. This suggests JNK does have some role in the cellular response to ischemia. In contrast, JNK protein is down-regulated in mutant tissue after 2 hours of IS treatment compared to wild-type tissue also treated for 2 hours. Since less cell death is observed in mutant tissue, this data suggests JNK protein levels are dependent on CCRL2. A possible simplified pathway is CCRL2 signals JNK to activate caspase-3 which leads to apoptotic cell death. Important to remember is that caspase-3 protein is up-regulated in mutant tissue, but this increase is half of the increase seen in wild-type. In other words, CCRL2 is not the only signaling pathway activating caspase-3 during the

cellular response. However, since the absence of CCRL2 directly corresponds to a decrease in JNK protein levels, there is possibly little or no cross-talk of pathways at the JNK level. But this portion of the study is still incomplete, 14 hour and 2 hour data are incomparable since numerous activities and mechanisms occur within the 12 hour difference, and I lack caspase-3 data at 2 hours in mutant tissue.

In order to solidify the previously stated conclusions about JNK, I would need to obtain JNK data in mutant tissue after 14 hours of treatment as well as caspase-3 data in mutant tissue after 2 hours of treatment. To fully explore whether there is little or no cross-talk of signaling pathways at the JNK level, I would utilize JNK inhibitors in wild-type tissue. If my conclusion is correct, I would expect to see a level of activated caspase-3 similar to the level found in mutant tissue. Conversely, I could inhibit JNK in mutant tissue and expect to see no change in the levels of activated caspase-3 when compared to uninhibited mutant tissue. Despite the incompleteness of this data, it is clear that JNK plays an important role in contributing to cell death in cerebral ischemia.

CCRL2 expression on neurons, CMKLR1, and chemerin

Through immunohistochemistry, CCRL2 was found to be expressed on neurons, but not on astrocytes or microglial cells. The receptor CCRL2 was found to be to be expressed on mast cells and differentiated B cells, and

functioned by concentrating chemerin on the cell surface to facilitate CMKLR1 binding during inflammation. The expression of CCRL2 on neurons, and not an immune-related cell, strengthens the idea that CCRL2 contributes to ischemia-induced injury as neurons are among the most susceptible to cell damage and death. Additionally, a previous study has shown that JNK promotes apoptosis in neurons after cerebral ischemia (Li et. al. 2010). Altogether, this supports the idea that CCRL2 and JNK promote neuronal cell death after cerebral ischemia.

Lastly, I have shown that both chemerin and CMKLR1 protein are up-regulated in wild-type tissue after 14 hours of IS treatment. As explained earlier, a previous study has suggested chemerin binding to CMKLR1 promotes chemotaxis of dendritic cells and macrophages during inflammation. As inflammation is characteristic of stroke, this finding is expected. Another study has shown that the chemerin and CMKLR1 duo promotes phagocytosis and efferocytosis to help resolve inflammation (Cash et. al. 2010). More work is required to study how CCRL2 might factor into this mechanism between chemerin and CMKLR1. As CCRL2 was thought to be a non-signaling receptor, serving to concentrate chemerin for CMKLR1, it would be interesting to study if CCRL2 holds the same role in a cerebral ischemic context. To this end, I would study chemerin and CMKRL1 expression in CCRL2 knock-out tissue.

Future directions

In this study I have shown CCRL2 promotes neuronal cell death in an *in vitro* model of cerebral ischemia, via activated caspase-3 and that JNK is most likely an intermediate in the signaling pathway between CCRL2 and apoptotic cell death. Further clarification of this mechanism would be invaluable to delaying irreversible neuronal cell death after a stroke incident by providing possible therapeutic targets.

IV:

Materials and Methods

Organotypic cortical slice cultures

Animal use was approved by the Institutional Animal Care and Use Committee of the University of California, San Diego. C57/Bl6 mice (Charles River Laboratories) or transgenic mice (CCRL2$^{-/-}$) of age 3 – 4 days old were used. The brains were removed and transferred into ice-cold dissection medium (Gey's balanced salt solution supplemented with D-glucose 6.5mg/mL). Cortices were cut transversely into slices of 300 μm using a Vibratome^{TM} 800 – McIllwain Tissue Chopper (Vibratome). Slices were transferred onto 30 mm Millicell-CM tissue culture inserts (Millipore) and placed in 35 mm culture dishes containing culture medium (Eagle medium (50%), Earle's balanced salt solution (25%), horse serum (25%), L-glutamine (1 mmol/L), penicillin/streptomycin (50 U/mL), and glucose (36 mmol/L)). Cultures were maintained in a 5% CO_2, 37°C incubator for 2 weeks before experiments were performed. Culture medium was half-replaced the second day after plating and every 3 days thereafter until the day of treatment. Chemicals used in the above media were obtained from Invitrogen or Sigma.

Quantification of Cell Death

Quantification was performed by Juan Wang, a lab technician in Dr. Haddad's lab. 5 μg/mL propidium iodide (PI) was added into the culture medium 24 hours before any treatment and kept at the same concentration through the experiment. PI fluorescence was observed on an inverted microscope equipped with a rhodamine filter set that has a 540-552 nm band-pass filter for excitation

and a 590 nm long-pass filter for emission (Zeiss Axiovert 200M microscope,

Zeiss) and the attached 12 bit CCD camera (C4742, Hamamatsu) were routinely

used for image acquisition. The light source, microscope and the camera were

controlled by a computer (Universal Imaging Corporation). For data collection,

the parameters of the microscope such as light intensity for excitation, exposure

time, camera gain, etc. were kept constant. Images were acquired and analyzed

with MetaFlour imaging-processing software (Universal Imaging Corporation).

The fluorescence intensity was measured offline in the hippocampal CA1, CA3,

and DG regions and the mean fluorescence intensity was expressed as MFI

(Rytter et al. 2003). Time-lapse imaging in brain slices was performed on an

Olympus BX61-WI with an FV300 confocal scanhead retrofitted for 2-photon

microscopy with a Wideband MaiTai ti: sapphire laser (Newport/SpectraPhysics)

tuned at 950nm. 60X time-lapse z-stacks were taken using a 1.1 NA dipping lens

every 15 minutes. The microscope was enclosed in a custom-made incubation

chamber and maintained at 37°C. A tent was built around the culture dish and

objective using wire and parafilm to provide an enclosed space for constant

infusion of 15% CO_2 and 1.5% O_2.

Induction of cell death with ischemic solution and total protein extraction

On day of treatment, slices were exposed to either (i) ACSF (NaCl: 129

mmol/L, KCl: 5 mmol/L, $CaCl_2$: 1.3 mmol/L, $MgCl_2$: 1.5 mmol/L, $NaHCO_3$: 21

mmol/L, glucose: 10 mmol/L, 315 mOsm, pH 7.4) or (ii) IS (Table 1). The

ischemic solution model was validated in previous study (Yao et. al. 2007). All of the above chemicals were obtained from Sigma.

Cortical tissue slices from 2 – 3 different animals were pooled and placed in ice-cold protein isolation buffer (Tris: 50 mmol/L, NaCl: 150 mmol/L, SDS: 0.1%, Na-deoxycholate: 0.5%, Triton-X 100: 1%, 1 tablet/50 mL of complete protease inhibitor cocktail tablets (Roche Diagnostics), and 230 µmol/L PMSF, pH 7.5) for extraction.

Membrane preparation

Tissue in protein isolation buffer were homogenized by 10 – 20 strokes with a hand-held plastic homogenizer. The homogenate was then centrifuged at 3,300 g for 10 minutes to remove cellular debris. The supernatant was separated and centrifuged at 27,000 g for 45 minutes. The supernatant was removed and stored at -80°C until used.

Western blot analysis

Total protein (30µg) was resolved on 10% precast NuPAGE Bis-Tris gels (Invitrogen) and electrotransferred onto polyvinylidene difluoride membranes (Immobilin-P, Millipore). Membranes were then incubated in blocking buffer (5% nonfat dry milk (Carnation, Nestle Food) in PBS (NaCl: 148.9 mmol/L, NaH_2PO_4: 2.8 mmol/L, Na_2HPO_4: 7.2 mmol/L, pH 7.4) with 0.1% Tween 20 for 1–2 h to block nonspecific proteins. The membranes were then incubated overnight at 4°C in the appropriate buffer containing one of the following primary antibodies

against: CCRL2, phosphorylated JNK, total JNK, cleaved caspase-3, chemerin, CMKLR1. Protein signal detection was achieved with the ECL chemiluminescence system (Amersham). For normalization, membranes were stripped and reprobed with affinity-purified goat polyclonal antibody to actin at 1:500 dilution (Santa Cruz Biotechnology). Scanning densitometry of immunoblot films was performed on a Personal Densitometer SI scanner (Molecular Dynamics) and analyzed with the aid of ImageQuant image analysis software (Molecular Dynamics). Densitometry measurements of Western blots from each experimental group were obtained, and absolute values were normalized to actin.

Immunofluorescence staining in slice cultures

Immunofluorescence staining was performed by Dr. Robert Douglas, an assistant adjunct professor in Dr. Haddad's lab. The slice cultures were fixed in 4% *p*-formaldehyde for 6 h at 4℃ and then permeabilized with 1% Triton X-100 in phosphate-buffered saline (PBS) overnight at 4℃. Th e slices were incubated in 10% goat serum for 1 h before being treated for 3 days with antibodies against: NeuN, GFAP, Iba1, or CCRL2 in antibody diluent (Invitrogen) at 4℃. After several PBS washes, slices were mounted on slides with Prolong antifade reagent with 4′,6-diamidino-2-phenylindole (DAPI) (Invitrogen). Immunofluorescent images were obtained and analyzed using confocal microscopy (Olympus FV1000, Olympus America Inc., Center Valley, PA, USA).

Table 1. An *in vitro* model of ischemic stroke

Composition of ischemic solution (IS) and artificial cerebral spinal fluid (ACSF).

Ion concentrations are in mmol/L and gas concentrations are in percentages.

	ACSF	IS
K^+ (mM)	3	64
Na^+ (mM)	150	51
Cl^- (mM)	139	77.5
Ca^{2+} (mM)	1.3	0.13
Glutamate (mM)		0.1
Glucose (mM)	10	3
O_2(%)	21	1.5
N_2 (%)	Balance	Balance
CO_2 (%)	5	15
HCO_3^- (mM)	21	4

pH	7.4	6.4
Temp °C	37	37

Table 1 continued.
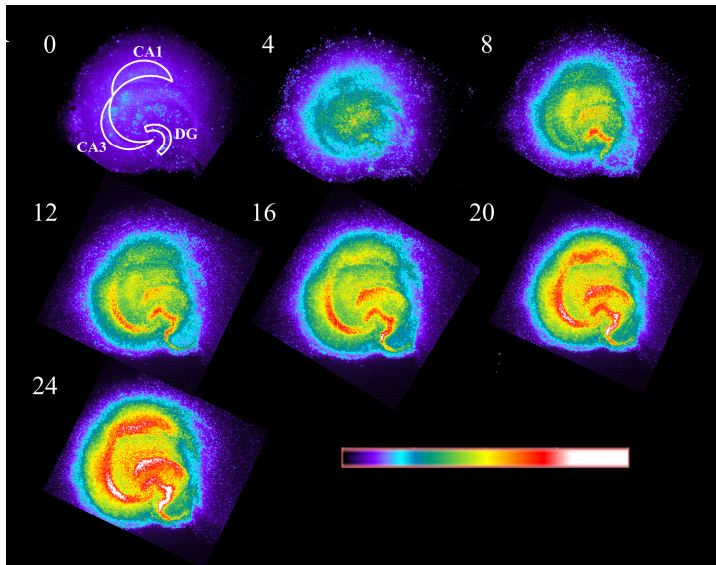
Figure 1. PI staining of hippocampal slices

Numbers on upper left of each image represent hours of IS exposure. The
pseudocolor scale is shown on the bottom right with purple indicating the least
and white the most intense levels of PI fluorescence.

Table 2. Microarray of up-regulated genes after 2 hours of IS treatment

Interleukin 1 beta is well-studied and its upregulation is expected. On the hand,

the upregulation of CCRL2 is novel.

List of IS-up-regulated genes			
Acc	Symbol	Fold Change	p Value
NM_008361	interleukin 1 beta **(Il1b)**	38.7	5.25E-56
NM_017466.	chemokine (C-C motif) receptor-like 2 **(Ccrl2)**	19.7	5.03E-53
NM_011198.	prostaglandin-endoperoxide synthase 2 **(Ptgs2)**	8.0	2.65E-40
NM_153553.	bHLH-PAS type transcription factor NXF **(Nxf)**	7.6	1.32E-39
NM_010554	interleukin 1 alpha **(Il1a)**	8.2	3.06E-37
XM_127883	immunoresponsive gene 1 **(Irg1)**	5.7	1.11E-35
NM_009841.	CD14 antigen **(Cd14)**	4.4	3.83E-34
NM_013693	tumor necrosis factor **(Tnf)**	5.8	4.70E-31
NM_008036	FBJ osteosarcoma oncogene B **(Fosb)**	3.5	2.64E-28
XM_127883.	immunoresponsive gene 1 **(Irg1)**	5.5	2.65E-27
NM_009140	chemokine (C-X-C motif) ligand 2 **(Cxcl2)**	3.4	8.12E-25
NM_010637.	Kruppel-like factor 4 (gut) **(Klf4)**	2.0	2.06E-11
NM_009856.	CD83 antigen **(Cd83)**	1.9	2.99E-11
NM_011905.	toll-like receptor 2 **(Tlr2)**	1.7	1.62E-08
XM_355746.	hypothetical protein 4732477G22 **(4732477G22)**	1.6	3.31E-07

A.
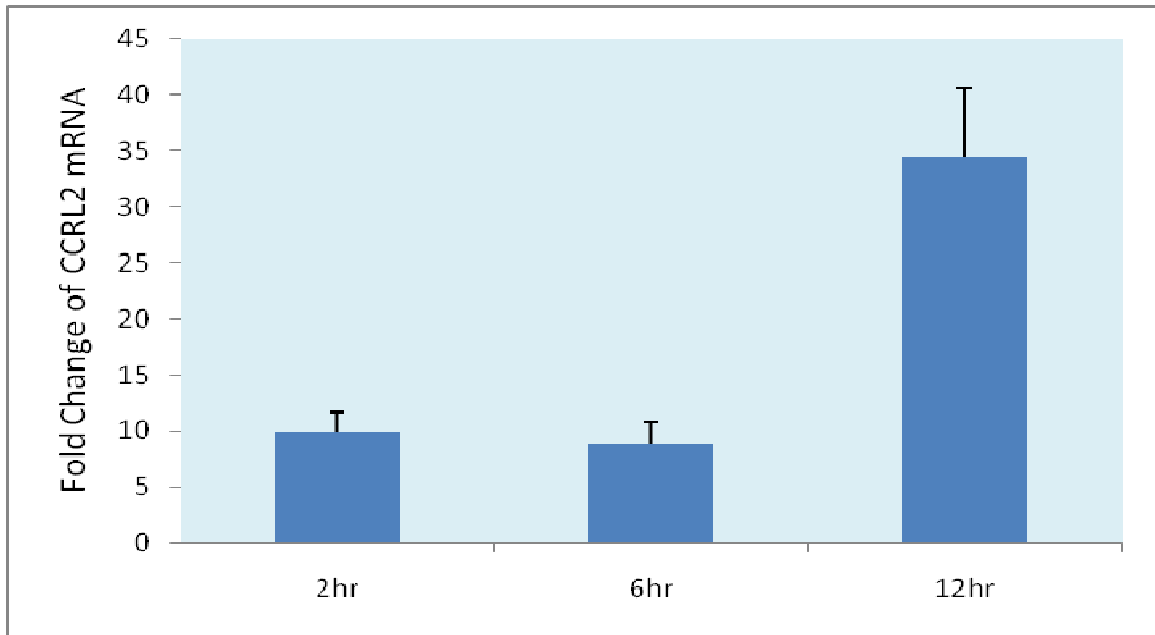
Figure 2. Expression of CCRL2 mRNA and protein after IS

(A) RT-PCR of wild-type cortical slices after 2, 6, and 12 hours of IS treatment. CCRL2 mRNA is significant increased at 12 hours compared to 2 and 6 hours leading to my evaluation of protein levels at 14 hours.

(B) Western blot of CCRL2 protein shows a significant increase in CCRL2 levels after 14 hours of IS treatment compared to ACSF.
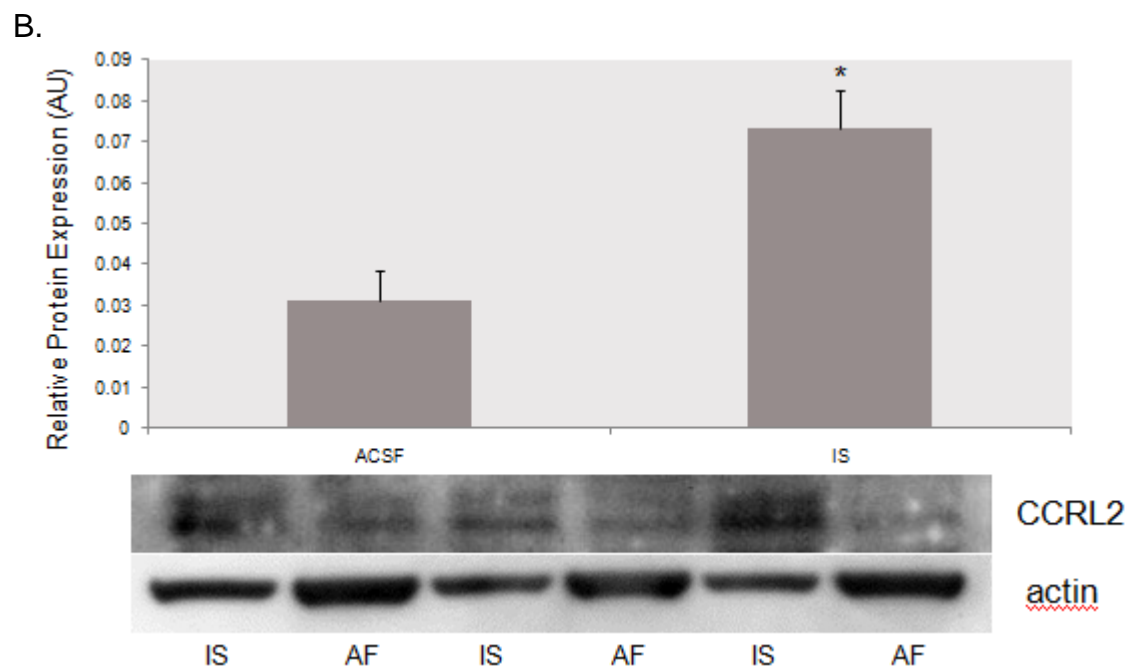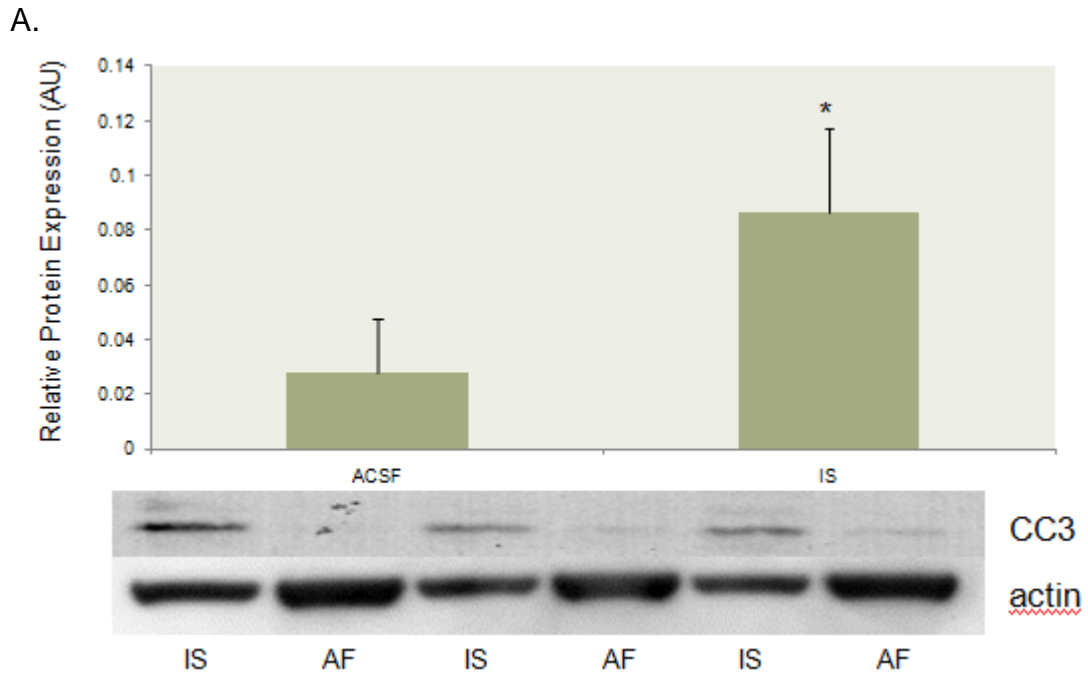
B.

Figure 2, continued

A.

Figure 3. Activated caspase-3 protein expression after IS treatment

(A) Activated caspase-3 showed a 6.42-fold increase in wild-type tissues after 14 hours of IS treatment.

(B) In mutant tissue, activated caspase-3 only showed a 3-fold increase after 14 hours of IS treatment.

B.
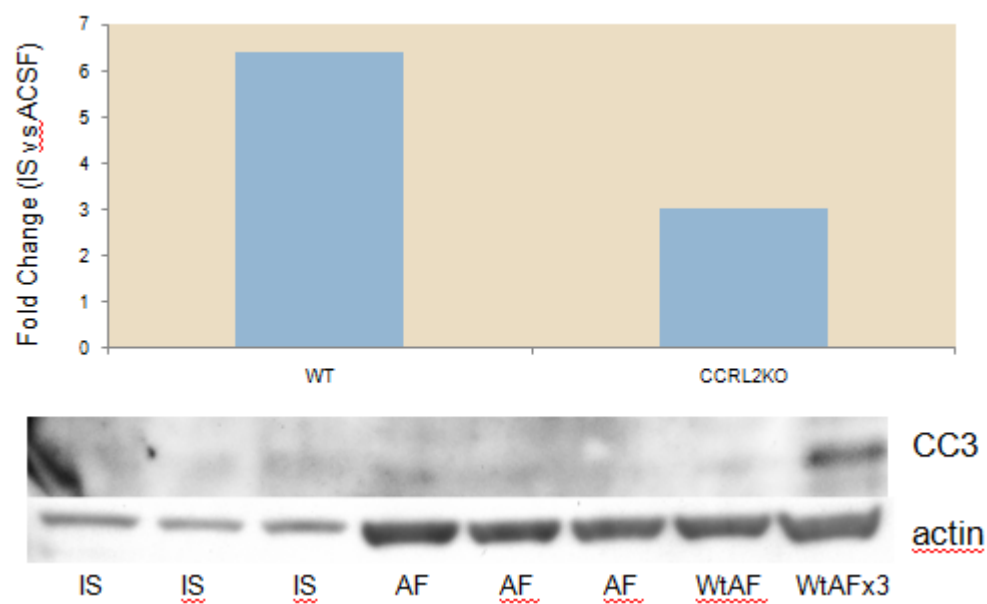
Figure 3, continued

A.
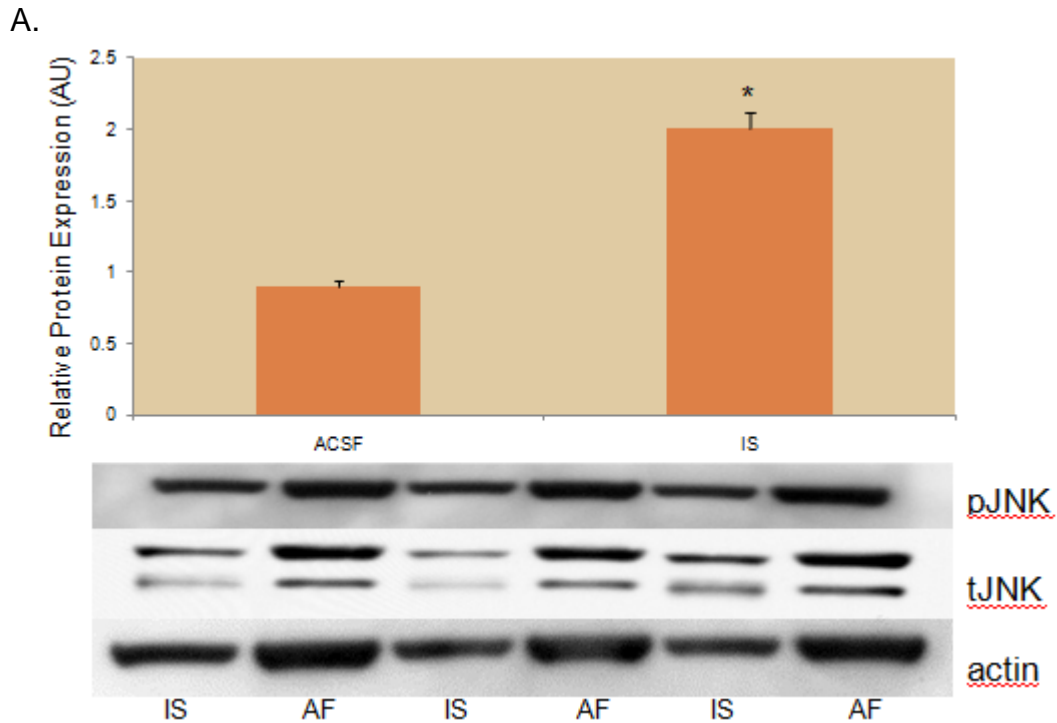
Figure 4. JNK expression after IS treatment

(A) Phosphorylated JNK is normalized to total JNK. The ratio of

activated/phosphorylated JNK is higher after IS treatment in wild-type tissue.

(B) Expression of activated JNK in CCRL2 KO tissue after 2 hours of IS

treatment.

(C) Expression of activated JNK in wild-type tissue after 2 hours of IS treatment.
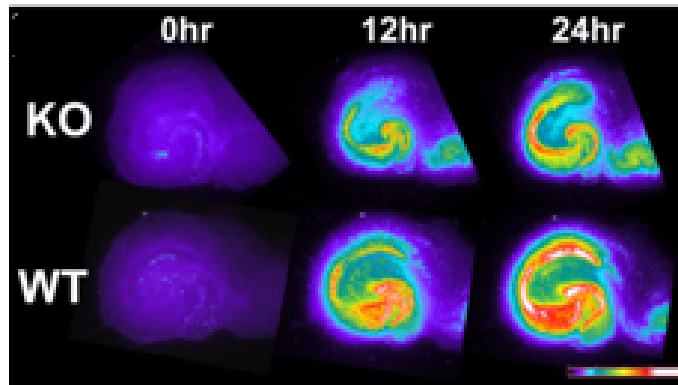
B.
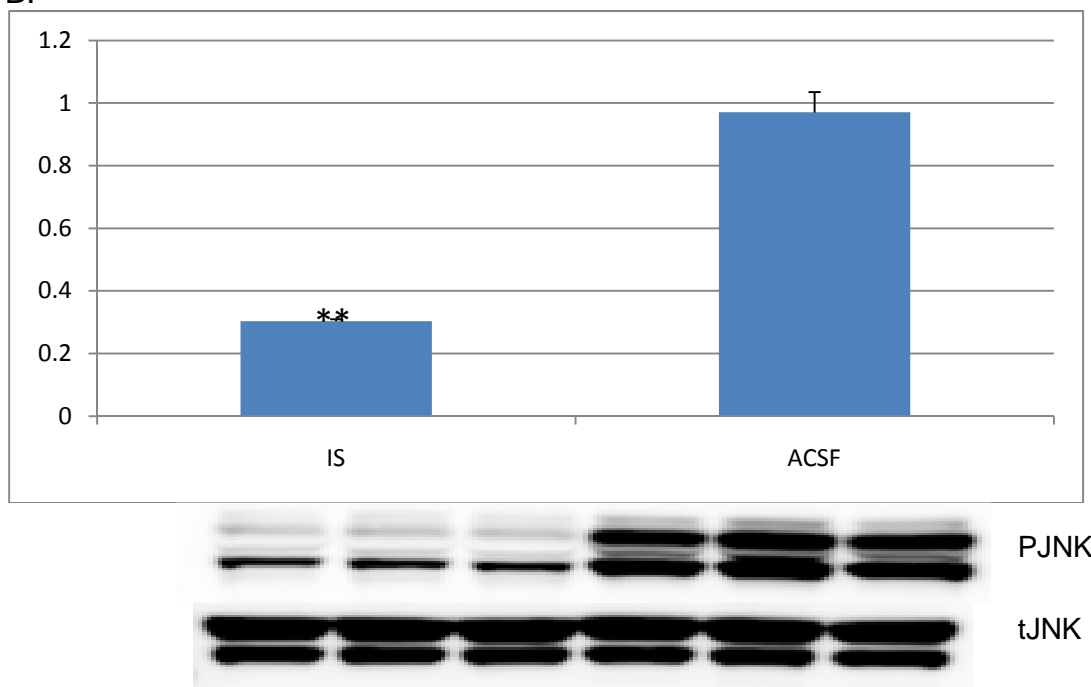
C.
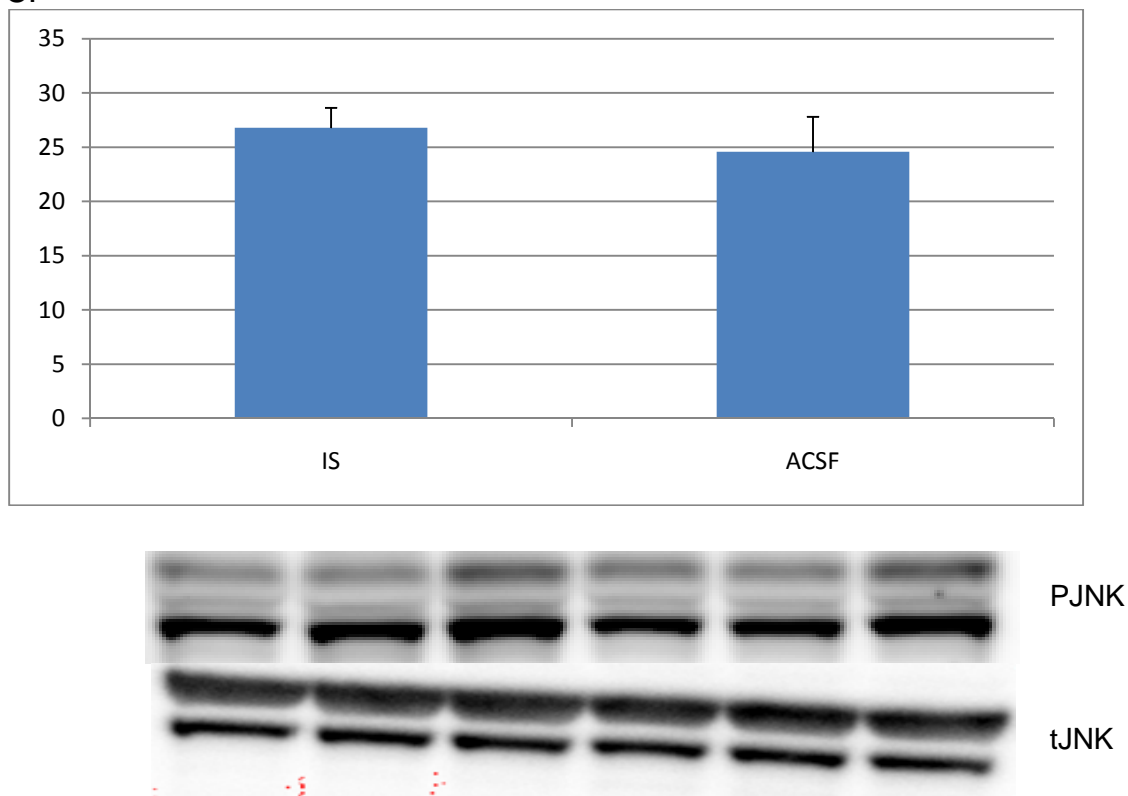
Figure 4, continued

A.

Figure 5. PI fluorescence in CCRL2 KO and wild-type hippocampal slices

(A) PI fluorescence in CCRL2 KO and wild-type tissue show significantly less fluorescence in mutant tissue compared to wild-type.
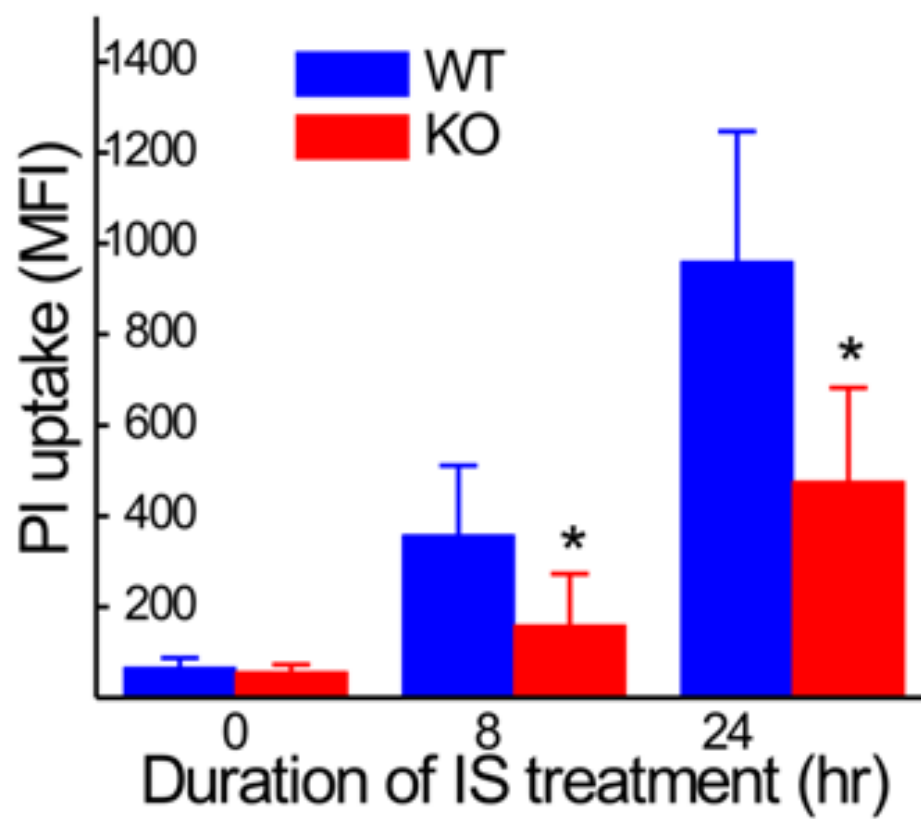
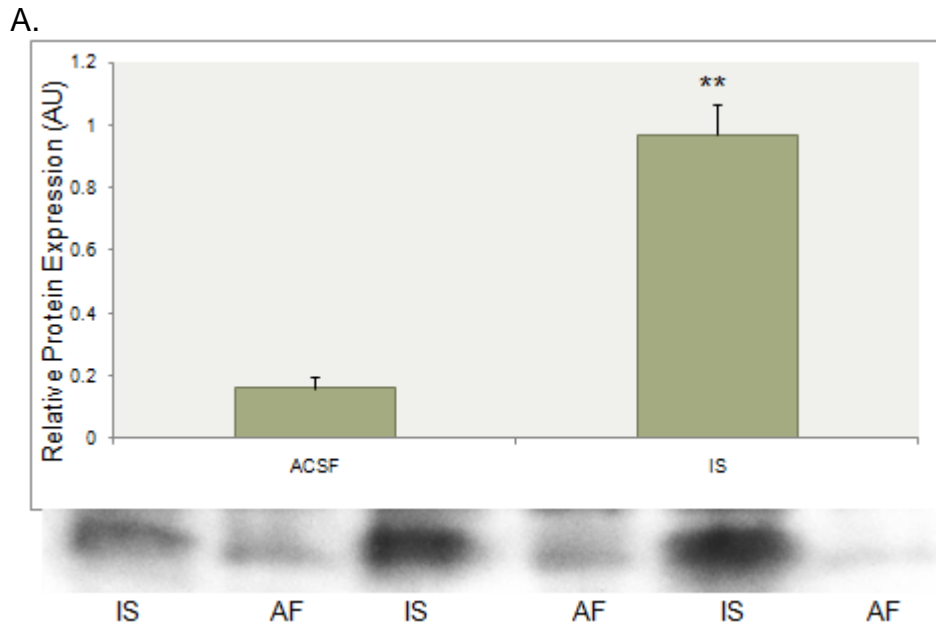(B) Quantification of (A).

B.

Figure 5, continued

A.

Figure 6. Expression of chemerin and CMKLR1/ChemR23 after IS treatment

(A) Expression of chemerin in wild-type tissue after 14 hours of IS treatment.

(B) Expression of CMKLR1/ChemR23 in wild-type tissue after 14 hours of IS
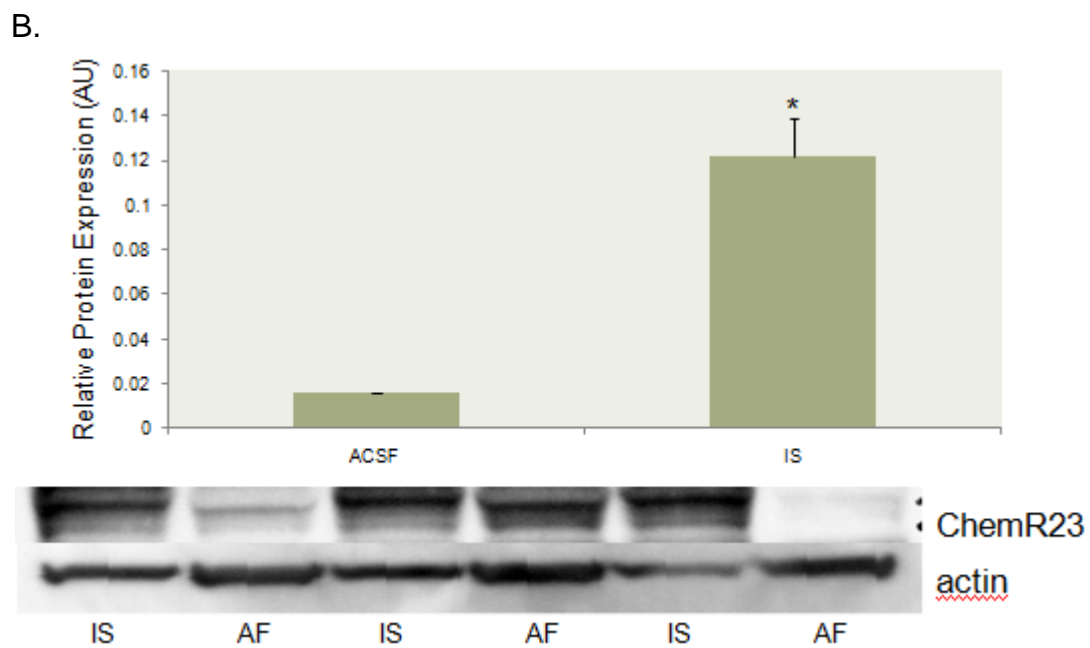
treatment.

B.

Figure 6, continued

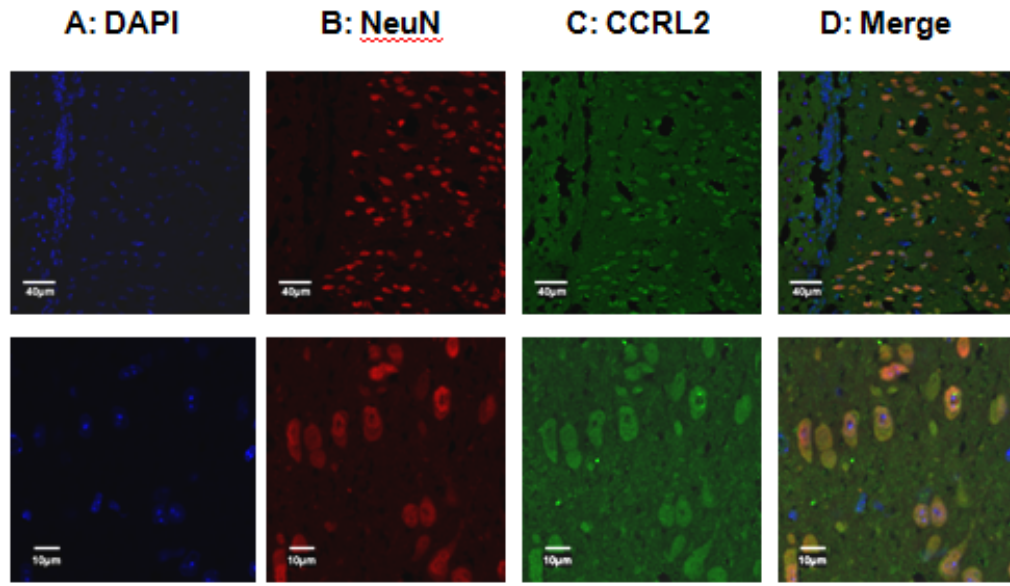**A: DAPI** **B: NeuN** **C: CCRL2** **D: Merge**

Figure 7. Location of CCRL2 expression

(A) – (L) Brain slices were removed from mice who had undergone middle cerebral artery occlusion (MCAO), an *in vivo* method of simulating stroke. Tissues were probed with antibodies for neurons, NeuN, astrocytes, GFAP, and microglial cells, Iba1. DAPI marked nuclei of living cells.
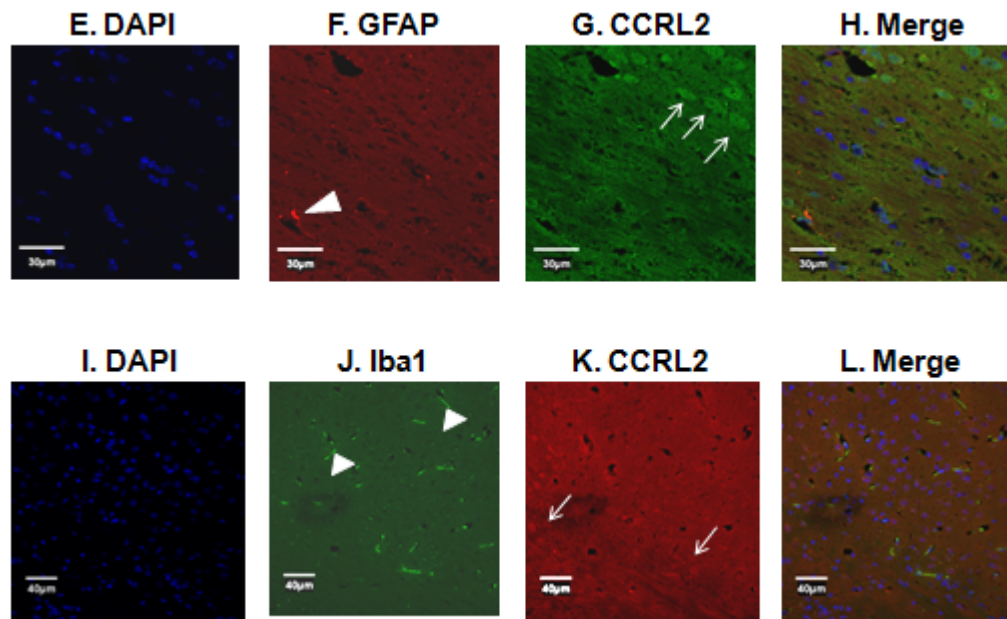
Figure 7, continued

V:
References

Back T, Hemmen T, Schuler OG. Lesion evolution in cerebral ischemia. J. Neurol. 2004; 251: 388-397.

Cash JL, Christian AR, Greaves DR. Chemerin peptides promote phagocytosis in a ChemR23- and Syk-dependent manner. J. Immunol. 2010; 184(9): 5315-24.

Fisher M. The ischemic penumbra: identification, evolution, and treatment concepts. Cerebrovasc. Dis. 2004; 17: 1-6.

Lecoeur H, Melki MT, Saidi H, Gougeon ML. Analysis of apoptotic pathways by multiparametric flow cytometry: application to HIV infection. Methods Enzymol. 2008; 442: 51-82.

Li J, Li Y, Ogle M, Zhou X, Song M, Yu SP, Wei L. DL-3-n-butylphthalide prevents neuronal cell death after focal cerebral ischemia in mice via the JNK pathway. Brain Res. 2010; 1359: 216-26.

Otero K, Vecchi A, Hirsch E, Kearley J, Vermi W, Del Prete A, Gonzalvo-Feo S, Garlanda C, Azzolino O, Salogni L, Lloyd CM, Facchetti F, Mantovani A, Sozzani S. Nonredundant role of CCRL2 in lung dendritic cell trafficking. Blood 2010; 116(16): 2942-9.

Mogoantă L, Pirici D, Pop OT, Bălşeanu AT, Rolea E, Dahnovici RM. Study of vascular microdensity in areas of cerebral ischemia on experimental model. Rom J Morphol. Embryol. 2010; 51(4): 725-31.

Rytter A, Cronberg T, Asztely F, Nemali S, Wieloch T. Mouse hippocampal organotypic tissue cultures exposed to in vitro "ischemia" show selective and delayed CA1 damage that is aggravated by glucose. J. Cereb. Blood Flow Metab 2003; 23: 23-33.

Yao H, Shu Y, Wang J, Brinkman BC, Haddad GG. Factors influencing cell fate in the infarct rim. J. Neurochem. 2007; 100(5): 1224-33.

Yao H, Sun X, Gu X, Wang J, Haddad GG. Cell death in an ischemic infarct rim model. J. Neurochem. 2007; 103(4): 1644-53.

Yoshimura T, Oppenheim JJ. Chemokine-like receptor 1 (CMKLR1) and chemokine (C-C motif) receptor-like 2 (CCRL2); two multifunctional receptors with unusual properties. Exp. Cell Res. 2011; 317(5): 674-84.

Zabel BA, Nakae S, Zúñiga L, Kim JY, Ohyama T, Alt C, Pan J, Suto H, Soler D, Allen SJ, Handel TM, Song CH, Galli SJ, Butcher EC. Mast cell-expressed orphan receptor CCRL2 binds chemerin and is required for optimal induction of

IgE-mediated passive cutaneous anaphylaxis. J Exp. Med. 2008; 205(10): 2207-20.